J|A|C|S
ARTICLES
Published on Web 05/16/2006

Self-Assembly of Peptide−Amphiphile Nanofibers: The Roles of Hydrogen Bonding and Amphiphilic Packing

Sergey E. Paramonov, Ho-Wook Jun, and Jeffrey D. Hartgerink*

Contribution from the Departments of Chemistry and Bioengineering, Rice University, 6100 Main Street, MS60, Houston, Texas 77005

Received January 25, 2006; Revised Manuscript Received April 7, 2006; E-mail: jdh@rice.edu

Abstract: The role of hydrogen bonding and amphiphilic packing in the self-assembly of peptide−amphiphiles (PAs) was investigated using a series of 26 PA derivatives, including 19 N-methylated variants and 7 alanine mutants. These were studied by circular dichroism spectroscopy, a variety of Fourier transform infrared spectroscopies, rheology, and vitreous ice cryo-transmission electron microscopy. From these studies, we have been able to determine which amino acids are critical for the self-assembly of PAs into nanofibers, why the nanofiber is favored over other possible nanostructures, the orientation of hydrogen bonding with respect to the nanofiber axis, and the constraints placed upon the portion of the peptide most intimately associated with the biological environment. Furthermore, by selectively eliminating key hydrogen bonds, we are able to completely change the nanostructure resulting from self-assembly in addition to modifying the macroscopic mechanical properties associated with the assembled gel. This study helps to clarify the mechanism of self-assembly for peptide amphiphiles and will thereby help in the design of future generations of PAs.

Introduction

Single tail peptide−amphiphiles[1−7] are a new class of biomaterials that, along with other peptide-based self-assembling nanomaterials,[8,9] are finding applications in many fields ranging from nanotechnology to tissue engineering. This is due to their ability to self-assemble into well-defined nanofibers, the chemical diversity which can be tolerated within this nanostructure, and their ease of synthesis. A typical PA molecule contains two regions: a hydrophobic aliphatic tail of a variable length and a hydrophilic peptide sequence attached to that tail through an amide bond. The tendency of the aliphatic tails to aggregate in aqueous solution is the driving force for self-assembly, while the peptide portion displays the active functional groups for particular applications. It has been found that for many single tail PAs the self-assembly leads to the formation of nanofibers, structurally similar to cylindrical micelles, in which the hydrophobic tails pack in the core of the fiber while the hydrophilic peptide is displayed on the fiber's surface. Depending on the sequence employed, the nanofiber can be covalently captured and their assembly can be controlled by pH or addition of multivalent cations.

Since the discovery of fiber forming, single tail, PAs, their self-assembly process was thought to occur mainly as a result of the hydrophobic interactions between aliphatic carbon tails.[3] Further investigations suggested that the β-sheet formation between the peptide region of a molecule may play a crucial role in directing the self-assembly into nanofibers as opposed to spherical micelles or vesicles.[1,2,10,11] Several theoretical works have also examined the role of electrostatic interactions in their self-assembly.[19] This observation is very important since it highlights the significance of a peptide secondary structure in the stability of the self-assembled nanofibers. Furthermore, if the entire peptide region is required to be folded in a β-sheet-type conformation, this may reduce the viability of the PAs as a biologically active matrix since biological signals are not only sequence sensitive but often require a specific peptide backbone

(1) (a) Behanna, H. A.; Donners, J. J. J. M.; Gordon, A. C.; Stupp, S. I. *J. Am. Chem. Soc.* **2005**, *127*, 1193−1200. (b) Ganesh, S.; Prakash, S.; Jayakumar, R. *Biopolymers* **2003**, *70*, 346−354. (c) Goeden-Wood, N. L.; Keasling, J. D.; Muller, S. J. A. G. *Macromolecules* **2003**, *36*, 2932−2938. (d) Paramonov, S. E.; Jun, H.-W.; Hartgerink, J. D. *Biomacromolecules* **2006**, *7*, 24−26.
(2) Beniash, E.; Hartgerink, J. D.; Storrie, H.; Stupp, S. I. *Acta Biomat.* **2005**, *1*, 387−397.
(3) Hartgerink, J. D.; Beniash, E.; Stupp, S. I. *Science* **2001**, *294*, 1684−1688.
(4) Hartgerink, J. D.; Beniash, E.; Stupp, S. I. *Proc. Natl. Acad. Sci. U.S.A.* **2002**, *99*, 5133−5138.
(5) (a) Jun, H.-W.; Paramonov, S. E.; Hartgerink, J. D. *Soft Matter* **2006**, *2*, 177−181. (b) Löwik, D. W. P. M.; van Hest, J. C. M. *Chem. Soc. Rev.* **2004**, *33*, 234−245. (c) Niece, K. L.; Hartgerink, J. D.; Donners, J. J. J. M.; Stupp, S. I. *J. Am. Chem. Soc.* **2003**, *125*, 7146−7147.
(6) Silva, G. A.; Czeisler, C.; Niece, K. L.; Beniash, E.; Harrington, D. A.; Kessler, J. A.; Stupp, S. I. *Science* **2004**, *303*, 1352−1355.
(7) Yu, Y.-C.; Tirrell, M.; Fields, G. B. *J. Am. Chem. Soc.* **1998**, *120*, 9979−9987.
(8) (a) Petka, W. A.; Harden, J. L.; McGrath, K. P.; Wirtz, D.; Tirrell, D. A. *Science* **1998**, *281*, 389−392. (b) Ghadiri, M. R.; Granja, J. R.; Milligan, R. A.; McRee, D. E.; Khazanovich, N. *Nature* **1993**, *366*, 324−327. (c) Pandya, M. J.; Spooner, G. M.; Sunde, M.; Thorpe, J. R.; Rodger, A.; Woolfson, D. N. *Biochemistry* **2000**, *39*, 8728−8734. (d) Haines, L. A.; Rajagopal, K.; Ozbas, B.; Salick, D. A.; Pochan, D. J.; Schneider, J. P. *J. Am. Chem. Soc.* **2005**, *127*, 17025−17029. (e) Lamm, M. S.; Rajagopal, K.; Schneider, J. P.; Pochan, D. J. *J. Am. Chem. Soc.* **2005**, *127*, 16692−16700. (f) Bellomo, E. G.; Wyrsta, M. D.; Pakstis, L.; Pochan, D. J.; Deming, T. J. *Nat. Mater.* **2004**, *3*, 244−248. (g) Berndt, P.; Fields, G. B.; Tirrell, M. *J. Am. Chem. Soc.* **1995**, *117*, 9515−9522. (h) Paramonov, S. E.; Gauba, V.; Hartgerink, J. D. *Macromolecules* **2005**, *38*, 7555−7561.
(9) Dong, H.; Hartgerink, J. D. *Biomacromolecules* **2006**, *7*, 691−695.
(10) (a) Zhang, S.; Holmes, T.; Lockshin, C.; Rich, A. *Proc. Natl. Acad. Sci. U.S.A.* **1993**, *90*, 3334−3338. (b) Ganesh, S.; Jayakumar, R. *Biopolymers* **2003**, *70*, 336−345.
(11) Stendahl, J. C.; Rao, M. S.; Guler, M. O.; Stupp, S. I. *Adv. Funct. Mater.* **2006**, *16*, 499−508.

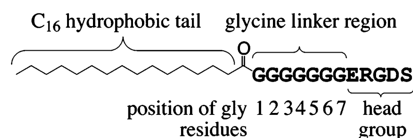

Figure 1. Schematic representation of PA **1**. The molecule includes three distinct regions: a hydrophobic alkyl tail, a glycine containing region, and a charged headgroup.

conformation. Nevertheless, several recent studies have demonstrated PA's excellent ability to serve as extracellular matrix mimics which promote cell adhesion, spreading, growth, motility, and differentiation.[2,6,12] In the present study, we elucidate the importance of hydrogen bonding for the stability of the nanofibers as well as their influence on the nanostructural morphology.

Peptide−Amphiphile Design. PA **1** is a prototypic peptide amphiphile containing a C_{16} hydrophobic alkyl tail and a 12 amino acid hydrophilic peptide (Figure 1). The peptide consists of a seven glycine linker region which connects the hydrophobic tail to the functional cell adhesion sequence. In this study, the headgroup of the synthesized PAs always contains the "ERGDS" (Glu-Arg-Gly-Asp-Ser) motif as an example of a bioactive adhesion sequence (RGDS) as well as glutamic acid to help control nanofiber formation by changing the pH or by adding multivalent cations. At neutral pH, the negative charges located on glutamate, aspartate, and the C-terminal carboxylate help to solubilize the PA, whereas at acidic pHs (below 4.5) or in the presence of Ca^{2+} ions, these charges are quenched, and the repelling forces are eliminated, allowing the self-assembly of the molecules to take place. In this study, we focus on the hydrogen bonding and conformation of the amino acids in the linker region. Our hypothesis is that amino acids located near the core of the PA nanofiber—that is, near the alkyl tail—will be more important for the self-assembly and final nanostructure as compared to those at the periphery. To test this, we prepared four different series of PAs consisting of 19 *N*-methyl glycine (sarcosine) derivatives (Table 1) and 7 alanine mutants (Table 2).

By selectively N-methylating an amino acid, we are able to prevent it from donating hydrogen bonds from the backbone amide. The hydrogen bonding network formed between self-assembled PAs can therefore be controlled and selectively interrupted by removing specific amide hydrogen atoms and substituting them with methyl groups. This allows us to control the self-assembly of the system as well as to direct it toward a particular nanostructure by managing the number and location of the allowed hydrogen bonds. By leaving only a certain number of hydrogen bonds, the effects of hydrogen bonding on the nanofiber formation and stability as well as overall PA morphology can be easily studied and evaluated. Three series of N-methylated derivatives were prepared. The first series (PAs **1**−**8**) starts by N-methylating a single glycine (PA **2**, position 7 in Figure 1) and moves toward the core adding one additional methyl group until all seven linker glycines are methylated. This lets us investigate the importance of the hydrogen bonding at the periphery of the nanofiber away from the hydrophobic core. We expect the amino acids in the interior of a nanofiber to play a more important role in stabilization than the amino acids situated on the outer regions since their conformational freedom is expected to be more restricted in the densely packed central regions. Therefore, the gradual methylation of the external amino acids should slowly decrease the stability of the self-assembled aggregate and eventually trigger a transition of the nanostructure or a complete failure to assemble. The methylation also allows us to understand the critical number of hydrogen bonds required for a successful nanofiber assembly. The second series (PAs **8**, **9**, and **15**−**19**) reverses the order of methylation as compared with series 1, starting with one N-methylated glycine at position 1 (PA **9**) and ending with seven N-methylated glycines at positions 1−7 (PA **8**). This series should confirm the importance of the core hydrogen bonding if the synthesized PAs fail to self-assemble into nanofibers and are not able to form hydrogels. It also helps us to distinguish between a simple number of hydrogen bonds required for assembly versus the positional effect of eliminating hydrogen bonds when compared to series 1. The third series (PAs **9**−**14** and **2**) contains one N-methylated glycine at each position through the glycine linker region. It should provide a probe for the relative importance of a hydrogen bond at a specific location for the nanostructure formation and resulting macroscopic physical behavior.

A fourth series of PAs was prepared to investigate the type of hydrogen bonding (Table 2). Again starting with PA **1** as a basis PA molecule, we made seven mutations in which alanine replaced one of the seven glycine linker amino acids. The alanine mutations start at the periphery of the nanofiber in position 7 (PA **20**) and move toward its core (PA **26**). Because glycine has no chiral center, the CD signal arising from this amino acid is relatively weak compared to that of alanine, thus alanine acts as a probe for the conformation of the PA in that particular location with only modest changes in the peptide chemical structure. Although the alanine mutation may have an effect on the conformation of the adjacent amino acids in addition to highlighting the local conformation, we believe that this series provides valuable insight into the secondary structure of the PA's backbone and the overall structure of the H-bonding network in the self-assembled PA nanofibers.

Results and Discussion

Mechanical Properties. The first series of PAs (PAs **1**−**8**) have increasing N-methylation and therefore a decreasing ability to form hydrogen bonds. The results of the mechanical studies indicated that only PAs **1**−**3** form stable hydrogels (as defined by G'/G'' being over unity at 10 Hz), while PA **4** forms a weak gel (Figure 2). In these PA molecules, up to three N-methylated glycine residues were introduced in the sequence next to the ERGDS headgroup at the positions 7, 6, and 5, respectively. The methylation of these residues prevents the formation of hydrogen bonds, and the resulting gels become weaker. This can be clearly seen in the values of storage modulus which decrease with increasing methylation. The introduction of each subsequent methylated glycine residue lowers the storage modulus (Figure 2), and methylation of three glycine residues (PA **4**, positions 5−7) results in a weak gel formation (which maintains its shape upon inversion but its mechanical properties cannot be reliably assessed with oscillatory rheology), indicating that the hydrogen bonding at these sites may be disrupted while the macroscopic physical behavior is maintained. In the case of PAs **5**−**8**, no gel formation was observed upon inducing the self-assembly either by lowering the pH or by adding Ca^{2+} ions.

(12) Jun, H.-W.; Virany, Y.; Paramonov, S. E.; Hartgerink, J. D. *Adv. Mater.* **2005**, *17*, 2612−2617.

Table 1. Summary of N-Methylated PA Prepared[a]

PA	Glycine Position 1	2	3	4	5	6	7	nanostructure	rheology
1	G	G	G	G	G	G	G	F	Gel
2	G	G	G	G	G	G	^{NMe}G	F	Gel
3	G	G	G	G	G	^{NMe}G	^{NMe}G	F	Gel
4	G	G	G	G	^{NMe}G	^{NMe}G	^{NMe}G	F	wGel
5	G	G	G	^{NMe}G	^{NMe}G	^{NMe}G	^{NMe}G	–	–
6	G	G	^{NMe}G	^{NMe}G	^{NMe}G	^{NMe}G	^{NMe}G	–	–
7	G	^{NMe}G	^{NMe}G	^{NMe}G	^{NMe}G	^{NMe}G	^{NMe}G	–	–
8	^{NMe}G	^{NMe}G	^{NMe}G	^{NMe}G	^{NMe}G	^{NMe}G	^{NMe}G	–	–
9	^{NMe}G	G	G	G	G	G	G	F	–
10	G	^{NMe}G	G	G	G	G	G	F	–
11	G	G	^{NMe}G	G	G	G	G	F	–
12	G	G	G	^{NMe}G	G	G	G	F	–
13	G	G	G	G	^{NMe}G	G	G	F	Gel
14	G	G	G	G	G	^{NMe}G	G	F	Gel
15	^{NMe}G	^{NMe}G	G	G	G	G	G	–	–
16	^{NMe}G	^{NMe}G	^{NMe}G	G	G	G	G	–	–
17	^{NMe}G	^{NMe}G	^{NMe}G	^{NMe}G	G	G	G	–	–
18	^{NMe}G	^{NMe}G	^{NMe}G	^{NMe}G	^{NMe}G	G	G	–	–
19	^{NMe}G	^{NMe}G	^{NMe}G	^{NMe}G	^{NMe}G	^{NMe}G	G	–	–

[a] 'F' indicates that the nanofibers were the dominant nanostructure present as observed by vitreous ice cryo-TEM; '–' means no fibers were present, and the sample was principally composed of spherical micelles and amorphous aggregates. For the column indicating rheology, options are Gel or wGel (weak gel), or '–' meaning no gel was formed.

Table 2. Sequences of the Synthesized PA Alanine Mutants[a]

PA	sequence	conformation of alanine
20	GGGGGG**A**ERGDS	polyproline type II
21	GGGGG**A**GERGDS	polyproline type II
22	GGGG**A**GGERGDS	polyproline type II
23	GGG**A**GGGERGDS	β-sheet
24	GG**A**GGGGERGDS	β-sheet
25	G**A**GGGGGERGDS	β-sheet
26	**A**GGGGGGERGDS	β-sheet

[a] All peptides were acylated at the N-terminus with palmitic acid. Position of the Ala residues is highlighted in bold. Conformation of the alanine was determined from difference CD measurements (Figure 4).

The second series of PAs (PAs **8**, **9** and **15**–**19**) that begins the N-methylation in the opposite direction (starting at position 1 and continuing to position 7 at the periphery of the PA) was similarly investigated. Mechanical testing indicated that none of the PAs in this series formed a stable gel upon induction of self-assembly. These data support the hypothesis of the high importance of the core hydrogen bonds for successful gel formation. In these PAs, the blocking of one hydrogen bond next to the hydrophobic core (position 1) prevents the gel formation. As expected, PAs in this series with additional methylation were also unable to form any gel. The mechanical testing data for the third series of PAs (PAs **9**–**14** and **2**) that contains only a single N-methylated glycine per PA indicated gel formation for PAs **13**, **14** (Figure SI-1), and **2** (Figure 2) and no gel formation for PAs **9**–**12**. These data are in excellent agreement with our hypothesis. Elimination of one hydrogen bond in the core region (position 1, 2, 3, or 4) disrupts the gel formation, while this elimination is tolerated in the periphery (positions 5, 6, and 7).

Together, these observations demonstrate that (a) blocking of hydrogen bonds at locations 5–7 reduces the strength of the resulting gel but does not eliminate it even when all three positions are blocked, and (b) blocking even a single hydrogen bond in locations 1–4 eliminates gel formation. The mechanical behavior of the hydrogels demonstrates that the interior region of the PA molecule plays an important role in defining the macroscopic physical properties of the material. This region is composed of two subregions that differ in the importance of the hydrogen bonding. The first subregion (core glycine residues in locations 1–4) is crucial for obtaining a gel, while in the second subregion (peripheral glycine residues in locations 5–7) hydrogen bonds are not required but when present increase the strength of the resulting gel.

TEM Studies. To obtain information about the effect of N-methylation on nanostructure, we performed vitreous ice, cryo-TEM studies (Figure 3). Vitreous ice cryo-TEM is the ideal method for investigating the structure of aqueous self-assembling materials because it is free from the large number of artifacts that arise upon drying, such as increased peptide and salt concentration among others. The cryogenic technique used in these studies allowed us to investigate the nanostructure of the sample at the conditions under which the samples were self-assembled without modifying their pH, or the concentration of the PA or Ca^{2+} during sample preparation. PAs **1**–**19** were assembled under identical conditions yet resulted in dramatically different nanostructures. Figure 3a–d (corresponding to PAs **1**–**4**) shows characteristic PA nanofibers with diameters of approximately 10 nm and with lengths between 0.3 and 2 μm. In sharp contrast, one can observe the formation of only spherical micelles in Figure 3e–h (corresponding to PAs **5**–**8**). This indicates that, contrary to initial assumptions,[3] the underlying geometry of the PA actually prefers spherical micelle formation when hydrogen bonding is eliminated and it is only in the presence of a hydrogen bonding network in which the cylindrical micelle-like nanofiber is preferred.

The second set of PAs (PAs **8**, **9** and **15**–**19**) was investigated by cryo-TEM as well. The results show that only PA **9** which has a single N-methylated glycine at position 1 forms nanofibers (Figure 3i). The rest of the set does not form nanofibers, and self-assembly leads only to the formation of micelles (Figures 3j and SI-3). This demonstrates again the critical importance of hydrogen bonding in the core region of the PA nanofiber. The molecules that contain more than one N-methylation in the region close to the hydrophobic core fail to form nanofibers.

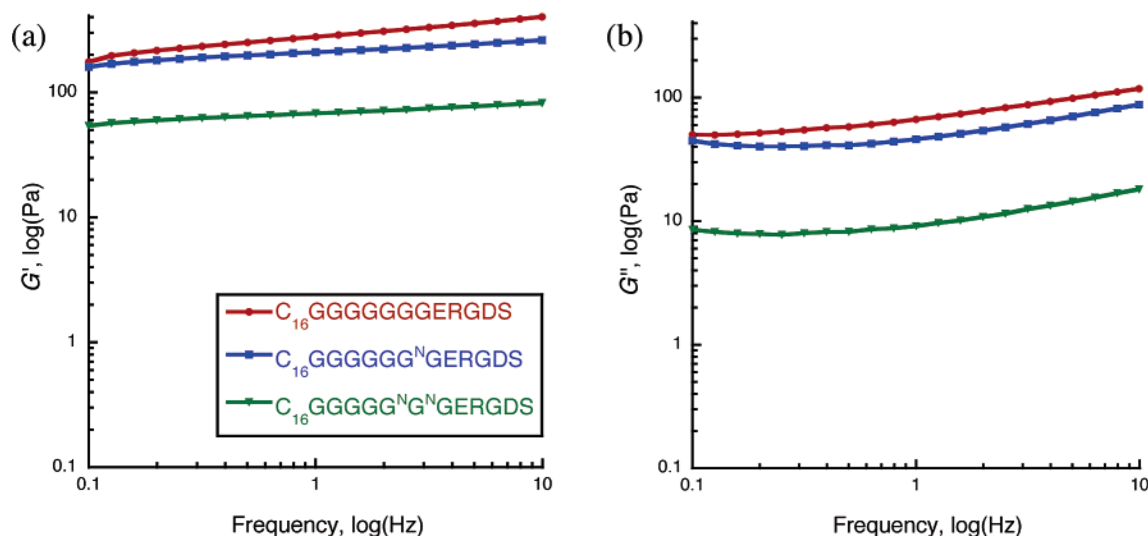

Figure 2. Oscillatory rheological data for PAs **1**–**3**. (a) Storage modulus (G'), (b) loss modulus (G''). $G' > G''$ demonstrates gel formation in each case. Gels were prepared at a concentration of 2 wt % of PAs.

This also demonstrates that a critical positional effect is being observed that cannot simply be attributed to the total number of possible hydrogen bonds. An important set of comparisons can now be made. With a single methylation at position 1 (PA **9**) versus position 7 (PA **1**), both materials form nanofibers, but only PA **1** forms a gel. In the case of methylations at positions 1 and 2 (PA **15**) versus 6 and 7 (PA **3**), PA **15** is unable to form fibers or a gel while PA **3** is able to form both. Similarly, methylation at positions 1–3 (PA **16**) versus 5–7 (PA **4**) reveals that PA **16** is unable to form fibers or a gel, while PA **4** is still able to form both.

The third series of PAs (PAs **9**–**14** and **2**) all form nanofibers when examined by cryo-TEM (Figures 3b,i and SI-2). One N-methylation is permitted for a PA to self-assemble into nanofibers, and the nanostructure does not depend on the position of the N-methylated residue in the sequence. Comparing this to our mechanical data, in which PAs methylated in positions 1–4 are not able to form gels while PAs methylated in positions 5–7 are, suggests that the strength, average length, quantity of nanofibers, and/or quality of cross links between these fibers must be reduced when methylation occurs in the critical core region.

The results of the cryo-TEM studies correspond well to the mechanical properties. Upon inducing the self-assembly, PAs **1**–**4** form nanofibers while PAs **5**–**8** form spherical micelles. Since PAs **5**–**8** do not self-assemble into any elongated aggregates, the material is not able to form a self-supportive hydrogel, whereas the formation of hydrogels in the case of PAs **1**–**4** results from the formation of nanofibers. These observations are also consistent with the sequence design of the PAs. PAs **5**–**8** contain anywhere from seven to four methylated residues in the glycine linker region. The methylation of the glycine residues close to the core of the nanofiber makes the nanofiber assembly unstable and favors the formation of spherical micelles which are held together primarily by hydrophobic interactions of alkyl tails. PAs **1**–**4** have zero to three methylated glycine residues in the sequence and are able to form from four to seven hydrogen bonds inside the glycine region. This has a dramatic impact on the nanostructure of the corresponding materials. When the PA is allowed to have these additional hydrogen bonds, the self-assembly is driven toward a formation of nanofibers as opposed to spherical micelles. The similar data for PAs **9** and **15**–**19** further support this conclusion. PA **9** contains only one N-methylated glycine residue at position 1. In this case, one core hydrogen bond was eliminated but the PA is able to form nanofibers. At the same time, it does not produce a stable gel. In PAs **15**–**19**, more than one core hydrogen bond was eliminated. The nanofiber formation is no longer possible, and the nanostructure is composed of spherical micelles and no gel formation is observed.

On the basis of the described data, including cryo-TEM studies and mechanical testing for PAs **1**–**19**, we may make the following conclusions: (a) one or more methylations of any glycines at positions 1–4 completely eliminate gel formation; (b) two or more methylations of glycines at positions 1–4 completely eliminate nanofiber self-assembly; and (c) methylating of 1, 2, or 3 glycines at positions 5–7 reduces gel strength but does not eliminate gel formation nor does it eliminate nanofiber self-assembly. Collectively, the stability of the self-assembled nanofibers and the mechanical properties of the corresponding materials strongly correlate with the nature and environment of the hydrogen bonding network within the nanofiber.

Evaluation of Nanostructure. As expected, hydrogen bonding plays a crucial role in a nanofiber formation. After blocking four hydrogen bonds, the energy of the remaining ones is not enough to hold the supramolecular aggregate together in the cylindrical micelle organization. Instead, the PA is only able to form spherical micelles. This also explains why single tail peptide–amphiphiles prepared previously,[7] which contained glycine-proline-hydroxyproline as the three amino acids closest to the alkyl tail, did not form nanofibrous structures. The proline and hydroxyproline amino acids prevent any chance for the formation of an extended hydrogen bonded network. These results illustrate that the nanostructure of a given PA may be manipulated by varying the position and number of hydrogen bonds that a given PA is allowed to form. One might expect that for any PA molecule that can potentially self-assemble into nanofibers there is a minimum number of hydrogen bonds necessary for the self-assembly to occur. It is also expected that by varying the number of hydrogen bonds the nanostructure of a PA can be switched between spherical and cylindrical

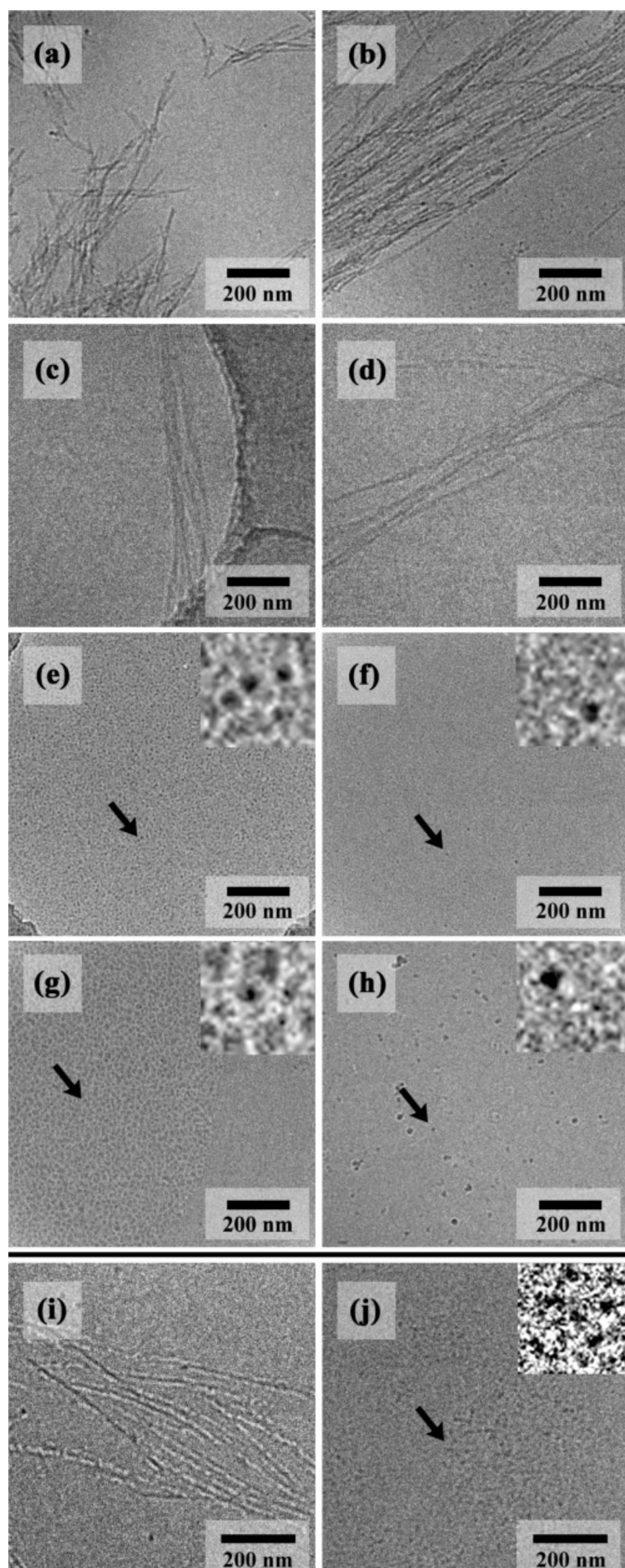

Figure 3. Vitreous ice, cryo-TEM images (a−h) of PAs **1**−**8**, respectively. The first four PAs form nanofibers upon inducing self-assembly with Ca^{2+}, while the remainder forms spherical micelles. (i) PA **9** has one N-methylated glycine at position 1 (close to the core) and forms nanofibers. (j) PA **15** has two N-methylated glycines at positions 1 and 2 and is not able to form nanofibers. Instead, micelle formation is preferred. Arrows indicate the location of insets.

assemblies. This nanostructural control is extremely valuable for isolating the effect of nanostructure versus chemical functionality on properties of interest, such as bioactivity. For example, a cell adhesion ligand can now be presented on a spherical or cylindrical nanostructure with minimal changes in chemical structure. This also suggests that a diversity of peptide secondary structures may be allowed at the fiber periphery as long as the core amino acids are allowed to adopt an extended β-sheet hydrogen bonding network.

PA Secondary Structure Investigation. Having determined which hydrogen bonds are critical in the formation of a PA nanofiber, we analyzed the conformation of the PA amino acids in each position of the peptide. To explore the secondary structure of the self-assembled PAs, we performed CD studies for the synthesized PAs. The CD spectra of PAs **1**−**3** displayed a polyproline type II helical coil conformation, while PAs **4**−**8** demonstrated a disordered conformation[9,13] with no indication of a β-sheet secondary structure (Figure SI-4). This, at first, appears surprising based on previous studies which indicate primarily β-sheet secondary structure in PAs.[2,4,11] It can be rationalized making two assumptions: being achiral, glycine contributes relatively little to the PA's CD spectra compared to the chiral amino acids in the ERGDS region, and the ERGDS sequence adopts a polyproline type II conformation. The peptide region of the synthesized PAs consists of a glycine segment, which lacks chiral centers and the ERGDS headgroup that contains four amino acids with chiral centers. Because of this, the glycine segment does not contribute significantly to the CD signal of the PA, and the observed CD spectra mostly result from the conformation of the PA's headgroup. Since, according to the mechanical studies, as well as cryo-TEM, the four hydrogen bonds near the core of the nanofiber are most important for self-assembly, it is not surprising that the rest of the peptide sequence may be permitted to adopt a weakly ordered, polyproline type II conformation. The residues close to the core of a nanofiber may still form β-sheet-type hydrogen bonds, but this signal will be weak since it occurs in the glycine region. To evaluate the validity of this argument, we synthesized a series of mutant peptides **20**−**26** (Table 2) containing one alanine residue at each position throughout the glycine linker region.

Because of alanine's chiral center, the CD spectra should disproportionately reflect the secondary structure at the alanine residue when compared to that of an equivalent glycine. The CD spectra for the PAs **20**−**23** (Figure SI-5) are complex and do not correspond to one simple type of secondary structure. This led us to assume that the observed spectra may represent a superposition of polyproline type II and a β-sheet-type spectra. This assumption is based on the fact that (a) the ERGDS headgroup of PAs adopts a polyproline type II conformation and (b) any signal from a single alanine residue is relatively small compared to the random coil signal from the ERGDS region. To overcome this problem, we subtracted the spectra of PA **1** from those of PAs **20**−**26**. The only optically active portion of PA **1** is the ERGDS headgroup, and it adopts a random coil conformation. PAs **20**−**26** have two optically active regions: the same randomly coiled ERGDS region and a single folded alanine residue. Assuming that the ERGDS spectrum

(13) (a) Quadrifolglio, F.; Urry, D. W. *J. Am. Chem. Soc.* **1968**, *90*, 2760−2765. (b) Horng, J.-C.; Raines, R. T. *Protein Sci.* **2006**, *15*, 74−83.

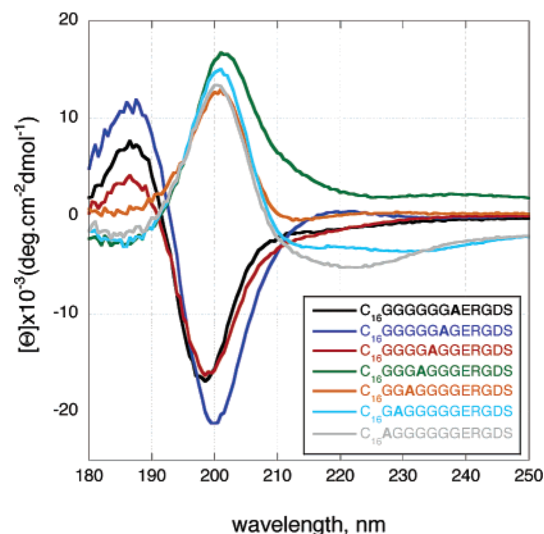

Figure 4. Difference circular dichroism spectra for the six alanine mutants (PAs **20**−**26**). The four alanine mutants closest to the hydrophobic core display a spectra most closely associated with parallel β-sheets with a minimum near 185 nm, a maximum near 200 nm, and a second minimum between 212 and 220 nm. The three alanine mutants distal from the core display a signal characteristic of polyproline type II secondary structure.

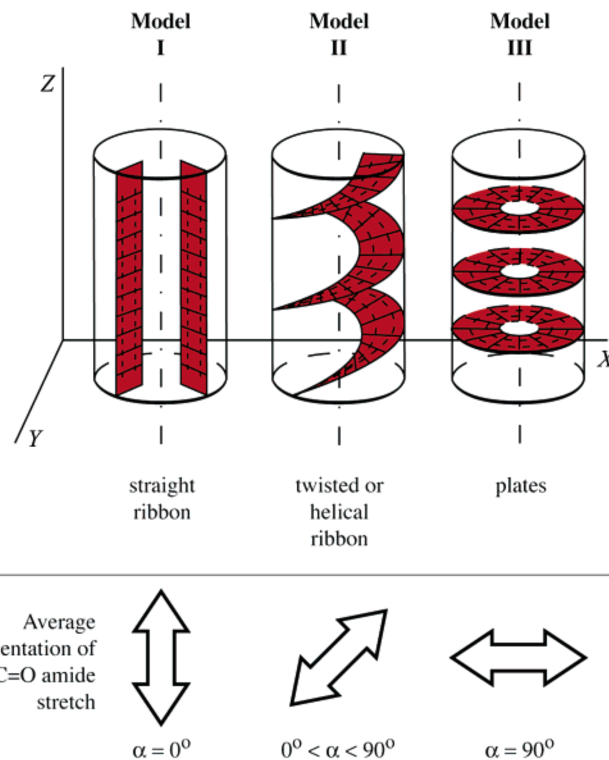

Figure 5. Schematic representation of the proposed β-sheet-type interactions along the PA nanofiber. Model I: H-bonding occurs in the planes oriented along the nanofiber Z axis. Model II: H-bonding takes place in a helical fashion of a variable pitch. Model III: H-bonding resides in the plates perpendicular to the nanofiber Z axis.

stays the same for all PAs, the result should primarily be the secondary structure at the alanine residue. The results of the subtractions are shown in Figure 4. They demonstrate that for the PAs **23**−**26** (when alanine is in positions 1−4) the CD spectra possess a minimum between 212 and 222 nm, a maximum near 200 nm, and a second minimum near 185 nm with the crossover point around 192 nm. Our observed data are very close to the CD signal produced by a β-sheet-like structure and are red shifted.[14] The red shift of the observed data together with crossover point at 192 nm indicates the presence of the parallel β-sheet structure which is consistent with the accepted model of a PA nanofiber. The conformation of the alanine residue in PAs **20**−**22** remains a random coil. In other words, the amino acids in positions 1−4 (Figure 1) that are close to the core of a nanofiber form hydrogen bonds with the adjacent peptide chains in a β-sheet conformation, while the amino acids in the periphery of the nanofiber are in a polyproline type II conformation.

The analysis of the CD data of alanine mutants matches the cryo-TEM and mechanical studies performed on the N-methylated PAs. These studies show that the sample morphology and nanostructure experience a drastic change after four hydrogen bonds have been blocked, which is reflected in the macroscopic mechanical properties. The CD data suggest that these four hydrogen bonds are formed as β-sheet-type interactions. PAs **1**−**4** form at least four core β-sheet hydrogen bonds, self-assemble into nanofibers, and form hydrogels, while PAs **5**−**8** and **15**−**19** form less than four hydrogen bonds, self-assemble into spherical micelles, and the viscosity of their solutions does not increase upon inducing self-assembly.

FT-IR Studies. To support the conformational findings, we performed IR studies for PAs **1**−**8** (Table SI-2). IR studies are complimentary to the CD studies since all amino acids give rise to the meaningful IR spectra and they do not depend on the optical chirality of a given amino acid residue. This allowed us to directly study the conformational state of the glycine residues at the positions 1−7. The observed IR spectra feature similar characteristics. All PAs except for PA **8** show two amide I bands near 1645 and 1636 cm^{-1}. PA **8** shows only one amide I band at 1652 cm^{-1}. Since, in case of PA **8**, all glycine residues are methylated and do not participate in hydrogen bonding, the amide I band corresponds to the randomly coiled ERGDS region. For the other PAs, the splitting indicates the presence of non-β-sheet regions (1645 cm^{-1}). Since the amide I region is a relatively crowded region,[15] we believe that the band at 1645 cm^{-1} combined with the observed CD spectra indicates the presence of a randomly coiled peptide region which arises from the presence of the ERGDS headgroup.[16] The band at 1636 cm^{-1} corresponds to β-sheet[17] type folded regions from the glycine residues located close to the core of a nanofiber. Thus, the results of IR studies provide additional evidence that the peptide portion of a PA molecule may be folded into two different conformations. The amino acids located in the interior of a nanofiber form hydrogen bonds which resemble parallel β-sheet-type interactions, while the amino acids situated on the outer regions are weakly organized.

Proposed Models of β-Sheet Interactions. The β-sheet interactions can be thought of occurring in one of three possible ways (Figure 5). The first possibility is depicted in model I. The cylinder represents a nanofiber, while the plane highlighted

(14) Sreerama, N.; Woody, R. W. In *Circular Dichroism: Principles and Appllications*, 2nd ed.; Berova, N., Nakanashi, K., Woody, R. W., Eds.; John Wiley & Sons: New York, 2000; p 878.

(15) Krimm, S.; Bandekar, J. In *Advances in Protein Chemistry*; Anfinsen, C. B., Edsall, J. T., Richards, F. M., Eds.; Orlando, FL, 1986; pp 181−364.
(16) Lazarev, Y. A.; Grishkovsky, B. A.; Khromova, T. B. *Biopolymers* **1985**, *24*, 1449−1478.
(17) Bandekar, J.; Krimm, S. *Biopolymers* **1988**, *27*, 909−921.

in red schematically represents the hydrogen bonded peptide network. Filled lines represent the orientation of the peptide, and dashed lines indicate the orientation of hydrogen bonds. The plane is not extended all the way to the center of the nanofiber since the core of the nanofiber is composed of the aliphatic tails. In model I, the peptide backbone amides form hydrogen bonds with one another parallel to the *Z* axis of a nanofiber. The preference for elongated self-assembled aggregates over other possible nanostructures can be explained by the propagation of hydrogen bonding along the *Z* axis of the fiber. Nonetheless, model I fails to describe the experimental fact that only four amino acids adopt a β-sheet-type conformation in the PA and the rest of the sequence appears to exist as a random coil. Since the distances between the individual peptide chains in one plane are virtually the same, it is reasonable to suggest that all the amino acids in the peptide backbone should participate in the β-sheet hydrogen bonding if model I is accurate.

In contrast, model III proposes that the β-sheet formation occurs in a cross section of a nanofiber in the *XY* plane. In this model, the β-sheet folding of only four amino acids, close to the core of a nanofiber, can be easily explained since the distance between the two adjacent peptide chains increases upon moving away from the center. Assuming this model, at some point, peptide backbones should be too far away to be able to form a hydrogen bond. Yet it is not clear how these layers are held together on top of each other, nor does it explain the strong preference for highly elongated nanofibers.

Therefore, it seems reasonable to suggest that the β-sheet-type interactions occur in a fashion that combines features of both models I and III. In model II, hydrogen bonds are formed in a helical way where the next peptide chain is shifted in the *Z* as well as *XY* direction. The shift in the *XY* direction causes the peptides to spread apart from one another toward the outside of the nanofiber while maintaining the general orientation of the hydrogen bond parallel to the fiber *Z* axis. Outer amino acids in the adjacent chains are too far away from each other to form hydrogen bonds, which is consistent with the fact that only four core amino acids participate in a β-sheet hydrogen bonding network. The helical hydrogen bonding network helps to maintain the nanofiber along its main axis and also participates in the radial stabilization of a supramolecular aggregate.

Grazing Angle and Transmission FT-IR Studies. To gain further insight into the structure of the hydrogen bonding network in the self-assembled nanofibers and to differentiate between the three proposed models, we performed additional IR studies, including grazing angle and oriented transmission experiments.[18] The key difference between the wo experiments is the relative orientation of the sample toward the incoming IR laser beam. In the case of the grazing angle IR, the beam comes almost parallel (10°) to the surface of the sample, whereas in the transmission IR, the orientation of the beam is perpendicular to the surface of the sample (Figure 6). This allows us to obtain and compare the IR spectra of the nanofibers oriented in two perpendicular ways. In both models I and II, the

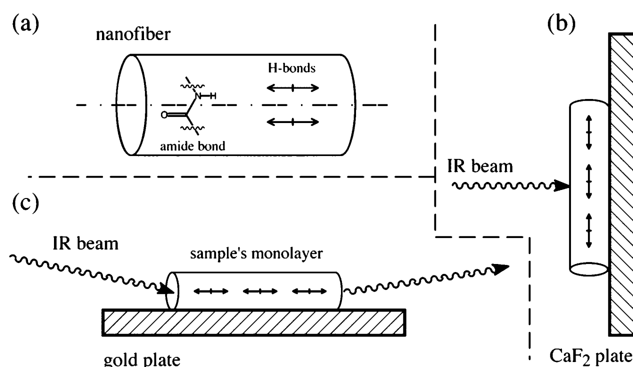

Figure 6. (a) Schematic representation of a relative orientation of amide bonds in a PA nanofiber. Orientation of the amide bonds and hydrogen bonds assumes model I. (b) IR beam comes perpendicular to the surface, nanofiber and amide bond in the case of transmission IR, and (c) almost parallel to the surface, nanofiber, and amide bond (10°) in the case of grazing angle IR.

orientation of the amide backbone carbonyl bond and its hydrogen bond to adjacent PAs is determined by the orientation of the PA nanofiber. In model I, the amide carbonyl is parallel to the nanofiber, while in model III, it is perpendicular. Because the PA nanofibers have an extremely high aspect ratio (length = 1000's of nm, diameter $\approx$ 10 nm), they will lie approximately flat when deposited on a surface. Thus by changing the orientation of the surface on which the PA fibers lie with respect to the IR beam, we can change the angle between the laser and amide bond. The IR spectrum of a peptide's amide bond can be broken into several regions, including the amide I band (between 1610 and 1690 cm^{-1}), which is primarily due to the C=O stretch, and the amide II band (between 1510 and 1560 cm^{-1}), which is primarily due to the out of plane bending of the amide's N–H and is oriented perpendicular to the amide I band.[15] Because of the above-described geometric constraints of the PA nanofiber and IR absorbances, the amide I band will be attenuated when the IR laser is oriented parallel to the C=O bond while the amide II is maximized. Conversely, when the IR laser is oriented perpendicular to the C=O bond, the amide I band will be maximized and the amide II band attenuated. Thus by depositing the PA nanofibers on a gold surface and performing grazing angle IR (Figure 6c) and by depositing PA nanofibers on a CaF_2 plate and performing standard transmission IR (Figure 6b), we are able to discern the orientation of the hydrogen bonds in a PA nanofiber and differentiate between models I and III.

If we assume model I, where the hydrogen bonds are oriented along the *Z* axis of a nanofiber, the grazing angle IR should attenuate the amide I band and enhance the amide II band since the incoming beam is parallel with the amide carbonyl bond (Figure 6c). The experimental results (Figure 7) show that this is indeed the case. The grazing angle IR spectrum shows a dramatic attenuation of amide I and relative enhancement of the amide II compared to transmission IR performed on CaF_2 plates. This indicates that the direction of the C=O bond coincides closely with the *Z* axis of a nanofiber, and therefore, it rules out model III, where the C=O double bonds are oriented perpendicular to the *Z* axis of a nanofiber. Nevertheless, these data are not able to distinguish between model I and model II. In both models, the entire C=O double bond vector, or a certain projection of it, lies along the *Z* axis of a nanofiber, and thus in both cases, the relative intensity of the amide II band will be

(18) Kim, H. S.; Hartgerink, J. D.; Ghadiri, R. *J. Am. Chem. Soc.* **1998**, *120*, 4417–4424.
(19) (a) Tsonchev, S.; Schatz, G. C.; Ratner, M. A. *Nano Lett.* **2003**, *3*, 623–626. (b) Tsonchev, S.; Schatz, G. C.; Ratner, M. A. *J. Phys. Chem. B* **2004**, *108*, 8817–8822. (c) Tsonchev, S.; Troisi, A.; Schatz, G. C.; Ratner, M. A. *Nano Lett.* **2004**, *4*, 427–431. (d) Tsonchev, S.; Troisi, A.; Schatz, G. C.; Ratner, M. A. *J. Phys. Chem. B* **2004**, *108*, 15278–15284.

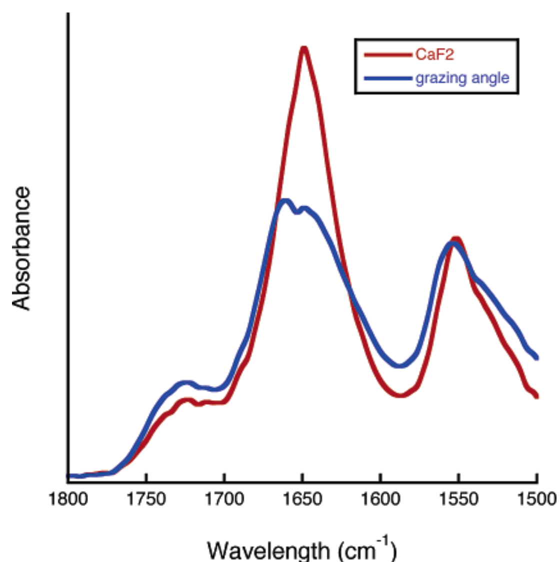

Figure 7. CaF_2 transmission IR versus grazing angle IR for PA **1**. The dramatic difference in the relative intensity of amide I and amide II bands can be clearly seen.

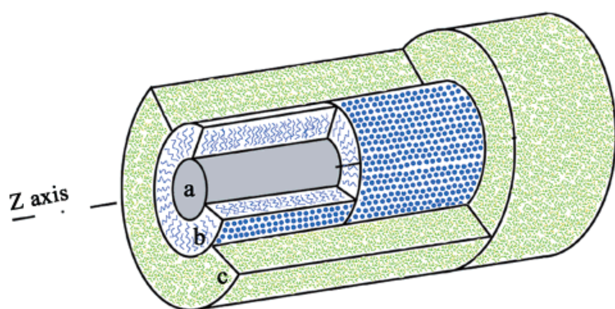

Figure 8. Three-dimensional representation of the regions of a PA nanofiber. Region (a) is the hydrophobic core composed of aliphatic tails. Region (b) is the critical β-sheet hydrogen bonding portion of the peptide and consists of four amino acids. Region (c) is the peripheral peptide region which is not constrained to a particular hydrogen bonding motif and forms the interface with the environment.

enhanced to some degree. We believe though that model II represents a more realistic description of a hydrogen bonding network in the nanofibers. This model accounts for the fact that (1) only a small number of amino acids participate in β-sheet hydrogen bonding and (2) it provides a basis for nanofiber axial stability and preference for elongation along the *Z* axis. The performed IR studies clearly eliminate model III and emphasize the importance of the hydrogen bonding in the nanofiber assembly. Model II allows for a wide variation in β-sheet hydrogen bonding orientation which in its extreme form is exactly model I where $\alpha = 0°$ or model III where $\alpha = 90°$. Without β-sheet hydrogen bonding, the self-assembly of the PAs leads to the formation of spherical micelles comprised of the inner hydrophobic core and the outer hydrophilic peptide shell. It is the formation of a hydrogen bonding network that alters the self-assembly and favors the organization of the PA molecules into nanofibers.

Conclusions

In the present paper, we prepared a series of modified PAs that allowed us to probe the molecular details of hydrogen bonding in peptide−amphiphile nanofibers and regulate their nanostructure and mechanical properties. It was found that the four amino acids closest to the core of the nanofiber form β-sheet hydrogen bonds oriented primarily down the *Z* axis of the nanofiber, and that disruption of these hydrogen bonds eliminates the ability of a PA to form an elongated, cylindrical nanostructure. Instead, the underlying geometric preference of the amphiphile reveals itself in the formation of spherical micelles, in contrast to initial expectations. The presence or absence of these hydrogen bonds allows us to select the nanostructure−spherical or cylindrical−that most suits the application at hand. It also allows us to prepare identical surface chemical functionality with dramatically different nanostructure and thereby differentiate between effects caused by one or the other. Amino acids further away from the core of the nanofiber are less restricted in their conformation, may accommodate a variety of nonpeptidic functionalities, and also play a less important role in stabilizing the nanostructure and macroscopic gel. This greatly increases the number of potential applications to which peptide−amphiphiles can be applied since accessing α-helical, β-sheet, collagen-like, or turn conformations may all be useful for particular applications. We believe that these findings will provide additional basis for the manipulations of the PA's nanostructure and will lead to the development of new tunable nanostructured materials.

Acknowledgment. J.D.H. gratefully acknowledges the Kinship Foundation for his Searle Scholar award. H.W.J. is thankful for his support by a Peter and Ruth Nicholas Postdoctoral fellowship. The authors gratefully acknowledge Prof. A. G. Mikos for the access to the AR 1000 Rheometer. This work was funded in part by the Robert A. Welch Foundation research grant number C1557.

Supporting Information Available: Detailed experimental section, including MALDI-MS data, cryo-TEM images, mechanical testing, CD and IR spectra. This material is available free of charge via the Internet at http://pubs.acs.org.

JA060573X